Available online at www.sciencedirect.com
ScienceDirect
Remote Sensing of Environment 109 (2007) 107–117
Remote Sensing of Environment
www.elsevier.com/locate/rse

A new spectrogoniophotometer to measure leaf spectral and directional optical properties

Didier Combes [a,*], Laurent Bousquet [b], Stéphane Jacquemoud [b], Hervé Sinoquet [c], Claude Varlet-Grancher [a], Ismaël Moya [d]

[a] INRA, UR4 Unité d'Ecophysiologie des Plantes Fourragères, BP 6, F-86600 Lusignan, France
[b] Etudes spatiales et planétologie, Institut de Physique du Globe de Paris — Université Paris 7, Case 89, 4 place Jussieu, 75252 Paris Cedex 05, France
[c] UMR547 PIAF, INRA, Université Blaise Pascal, F-63100 Clermont Ferrand, France
[d] Equipe Fluorescence et Télédétection, Laboratoire de Météorologie Dynamique, Ecole Polytechnique, 91128 Palaiseau Cedex, France

Received 11 August 2006; received in revised form 15 December 2006; accepted 16 December 2006

Abstract

In this paper we present a new spectrogoniophotometer (SGP) dedicated to the assessment of plant leaf bidirectional optical properties. It consists of a mechanical apparatus coupled with an imaging spectrometer using a bidimensional CCD photodetector. Unpolarized light fluxes are sampled at high spectral and directional resolution to provide biconical reflectance and transmittance factors, every nanometer from 500 nm to 880 nm and at 800 source-sensor configurations (four illumination directions by 200 viewing directions covering the whole sphere). From these calibrated measurements we derive the leaf Bidirectional Reflectance and Transmittance Distribution Functions (BRDF and BTDF). The angular-integrated quantities defined as the Directional Hemispherical Reflectance and Transmittance Function (DHRF and DHTF) are also calculated. The first three sections emphasize the instrumental and calibration issues, as well as the radiometric definitions. In the last section we present some experimental results acquired on various monocot and dicot leaves with special attention to surface reflection. The shape, position and magnitude of the specular lobe, which is a characteristic of many leaves in the forward direction, is investigated for beech (*Fagus sylvatica* L.) and laurel (*Prunus laurocerasus* L.) using a leaf BRDF model. The width of the specular peak is very variable according to the species and the illumination angle, as well as its contribution to the directional–hemispherical reflectance. Finally, implications in plant physiology or remote sensing are broached.

Keywords: Goniometer; Spectral; Bidirectional; Hemispherical; Reflectance; Transmittance

1. Introduction

Most radiative transfer models used in ecophysiology and remote sensing assume leaves to be Lambertian, i.e., perfect scatterers. It simplifies the radiative transfer equations and enables the use of hemispherical reflectance and transmittance spectra which are easy to measure (Myneni & Ross, 1991; Myneni et al., 1989). Consequently, the bidirectional properties of leaves as well as their spectral properties have received little investigation, although they may significantly influence several plant responses and remote sensing signals. First, the regulation of plant growth by photomorphogenesis depends on the perception of the light spectra at the organ level, and it has been proven that both the spectral and directional optical properties of plant leaves may affect the development of nearby plants (Ballaré et al., 1987). The perception process involves two families of photoreceptors, the phytochrome and the cryptochrome, located in the whole plant and sensitive to the red to far-red ratio and the blue wavelength domains, respectively (Smith, 1982). At least for the red bands, previous measurements (e.g., Breece & Holmes, 1971) have shown differential spectral responses of bidirectional leaf reflectance/transmittance, suggesting that the red to far-red ratio will show directional changes after interaction of radiation with a plant organ. Second, animal

* Corresponding author. INRA, UR4 Unité d'Ecophysiologie des Plantes Fourragères, BP 6, F-86600 Lusignan, France.
E-mail addresses: dcombes@lusignan.inra.fr (D. Combes), bousquet@ipgp.jussieu.fr (L. Bousquet), jacquemoud@ipgp.jussieu.fr (S. Jacquemoud), sinoquet@clermont.inra.fr (H. Sinoquet), ismael.moya@lmd.polytechnique.fr (I. Moya).

0034-4257/$ - see front matter © 2007 Elsevier Inc. All rights reserved.
doi:10.1016/j.rse.2006.12.007

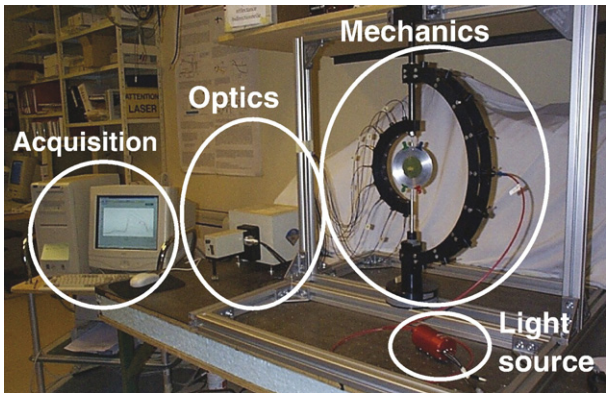

Fig. 1. Experimental device designed to measure leaf bidirectional optical properties.

vision is monitored from the perception of spectral radiation in two to four wavebands which may range from the ultraviolet to the near infrared (Stavenga, 2002). The combination of several bands allows the animal to detect particular plant organs, e.g. flowers by bees or fruit by birds. It might be possible that animals use the directional information to detect plant organs, even if there is no experimental evidence to date. Third and more important for readers, bidirectional optical properties of leaves are involved in remote sensing applications. The current generation of spaceborne sensors (e.g., CHRIS, MISR, or POLDER) that can measure the radiance of targets in several viewing angles also urge the scientific community to take an interest in this aspect of leaf optics, as suggested by recent workshops on multiangular remote sensing. Therefore the specular reflection at the leaf surface may affect the angular distribution of light inside and outside the canopy and consequently the interpretation of radiation measurements at all wavelengths (Grant et al., 1993). What determines the leaf BRDF/BTDF (Bidirectional Reflectance/Transmittance Distribution Function)? This question is still an issue, even though leaf surface characteristics are intuitively understood to be the main factor involved in these properties.

Although a number of studies have been devoted to leaf bidirectional properties (see the recent review in Von Schönermark et al., 2004), there remains a lack of commercial goniophotometers adapted to such measurements. This lack of bidirectional measurements is true for leaves but also for other translucent targets like fabric, paper, insect integument or human skin (e.g., Jacques et al., 1987; Pont & Koenderink, 2003). Various devices have been designed: in the simplest one, the leaf polarized reflectance is measured at the angle of incidence of 55° to the surface normal (Vanderbilt & Grant, 1986). At this particular angle called the Brewster angle, polarization allows separation of surface and sub-surface components of reflectance. In order to better sample the BRDF and/or BTDF, one or several detectors can be mounted on a rotation stage while the light source is fixed in position. Most of the goniophotometers are built this way, which allows measuring scattering in the principal plane (Brakke et al., 1989; Howard, 1971) or full light distributions (Walter-Shea et al., 1989). Sometimes however, it is just the opposite: the detectors are fixed and the light source is mounted on a rotation stage (Okayama, 1996). Finally, in other devices, all components are fixed (Sarto et al., 1989). In all reports, measurements are performed in the visible/near-infrared region, in one to several wavebands, and in polarized or non-polarized conditions, but very few of them combined both the spectral and directional dimensions. The latter is however crucial to better understand the determinism of leaf surface reflectance, as recently shown by Bousquet et al. (2005).

This paper describes a device designed to fill that gap and to measure leaf reflectance or transmittance every nanometer from 500 nm to 880 nm and at 800 source-captor configurations (four illumination zenith angles {5°, 25°, 45°, 65°} by about 200 viewing directions covering the whole sphere). The apparatus which uses a CCD bidimensional detector to simultaneously measure the spectral and directional variations of the scattered light is first depicted. Details for the derivation of bidirectional and directional–hemispherical quantities are then provided. We finally present measurements acquired during several experiments, emphasizing the nature of the

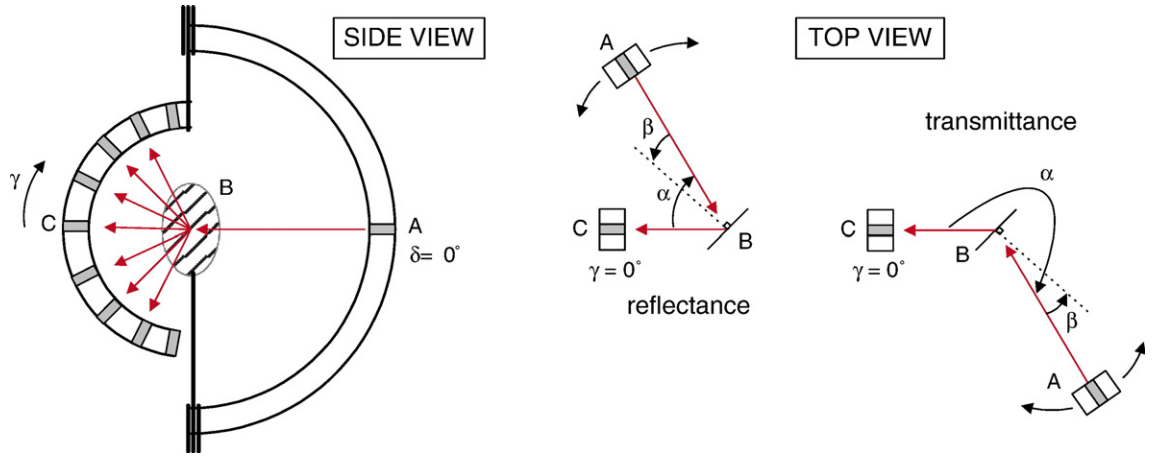

Fig. 2. Side view and top view of the spectrogoniophotometer: (A) outer arc holding the light source, (B) sample holder maintaining the sample (reference panel or leaf) vertically (see Fig. 3), (C) inner arc holding the seven viewing optical fibers of the detection system. The four angles α, β, γ, δ which characterize a particular measurement configuration are registered at each acquisition.

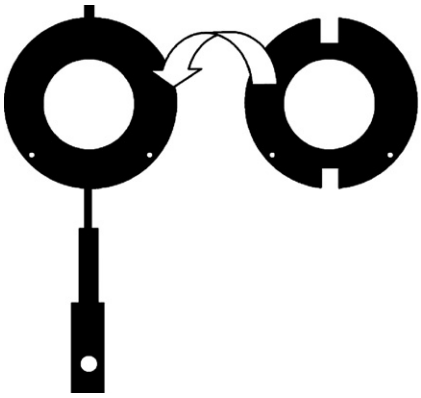

Fig. 3. Sample holder. The leaf is wedged between the two aluminum discs. The disc aperture is 50 mm across. A special sample holder (not shown) has been designed for the reference panel.

specular lobe which is distinctive of the BRDF of most leaf species.

2. Description of the apparatus

The spectrogoniophotometer (SGP) shown in Fig. 1 was developed by the *Institut National de la Recherche Agronomique* (Combes, 2002), the *Laboratoire pour l'Utilisation du Rayonnement Electromagnétique*, and the *Université Paris 7*. It was configured to make measurements of both leaf biconical reflectance and transmittance factors on vertically mounted samples.

2.1. Mechanics

The SGP consists of two aluminum coaxial arcs (diameter 200 mm and 480 mm) moving around a common diametrical and vertical axis (Fig. 2). All components likely to be exposed to the light source are coated with a black mat paint and are mounted on an oversized frame to guarantee stability. In order to avoid surrounding light interference, the SGP was enclosed in a black box (not shown in Fig. 1). Nine radial holes were drilled every 20° along the inner arc to support the nine optical fibers of the detection system (position indicated by the angle γ). However, the two extreme fibers at grazing viewing angles were not used due to a very low signal-to-noise ratio and to geometrical misalignments. The outer arc also presents seven holes evenly spaced at 20° in which an illumination optical fiber can be positioned (angle δ usually set to zero degree). At the center of the two arcs, a sample holder maintains the leaf gently pressed between two aluminum discs (Fig. 3). The holder was designed for leaves but also for reflectance standards of about 30 mm wide. A bevelled-edge circular aperture at the center of each disc allows the illumination beam to light the leaf surface without shading. The sample holder and the outer arc are interdependent, i.e. they turn together (angle α) to change the viewing directions while the inner arc is fixed in position. The SGP was designed this way to prevent the optical fibers from twisting (e.g., Sasse, 1993), because twist effects may change fiber transmission capacity. In order to allow measurements in the principal plane for various incidence angles, the sample holder is rotated by steps of 20° (angles β of 5°, 25°, 45°, and 65°). The four angles α, β, γ and δ defining the system native coordinates are read on the graduated arcs attached to the SGP. A mathematical conversion is required to obtain the light source (subscript 's') and viewing (subscript 'v') directions provided as usual spherical angles (θ, ϕ):

$$\begin{cases} \theta_s = arcos(\cos\delta \times \cos\beta) \\ \phi_s = \arctan\left(\dfrac{\sin\beta}{\tan\delta}\right) \\ \theta_v = arcos(\cos\gamma \times \cos(\alpha+\beta)) \\ \phi_v = \arctan\left(\dfrac{\sin(\alpha+\beta)}{\tan\gamma}\right) \end{cases} \quad (1)$$

2.2. Optics

The source of illumination is a tungsten halogen lamp (HL-2000, Ocean Optics) delivering 17 mW of unpolarized light. It is coupled with a 600 μm core quartz optical fiber, the output of which is focused by a plano-convex lens (focal length 15 mm, diameter 10 mm) on the center of the sample holder. The illumination beam is parallel and forms a spot of 7 mm across on the sample at nadir. The solid angle subtended by the source is $\Omega_s = 7 \cdot 10^{-4}$ sr. Seven optical fibers with a core diameter of 100 μm and a numerical aperture of 0.22 collect the reflected or transmitted light at the very same moment, which speeds up the acquisition time. They are coupled with plano-convex lenses similar to the one above-mentioned and image the center of the sample holder. The viewing beams are set to parallel which leads to a viewed area at nadir of 7 mm across. The solid angle subtended by the detectors is $\Omega_v = 7 \cdot 10^{-3}$ sr. Geometry of light beams can be modified by changing the distance between the optic fibers and their corresponding lenses.

The collecting fibers are mounted together on a multileg optical system which matches the rectangular entrance slit of the imaging spectrometer *via* a mirror-based imaging fiber adapter (Horiba Jobin-Yvon). Active fibers are separated from each other by dead ones in order to avoid spatial mixing in the spectrometer (Fig. 4). In this setup we used the compact TRIAX 180 imaging spectrometer (Horiba Jobin-Yvon) characterized by a 180 mm focal length, an input aperture of f/3.9, and a 100 gr mm^{-1} grating, with a dispersion of 43 nm mm^{-1}. The

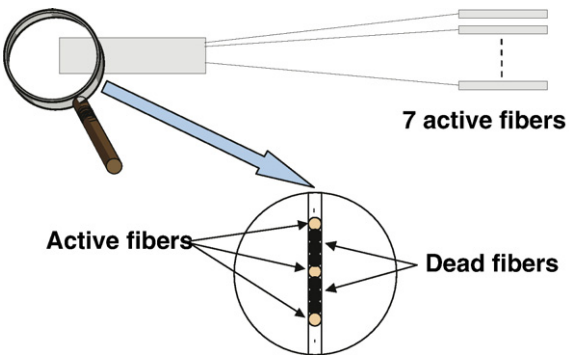

Fig. 4. Multileg optical fiber.

actual spectral resolution is defined by the width of the 100 μm entrance slit (diameter of the fiber-core). The spectrometer is interfaced to an air-cooled CCD detector system (Spectrum One, Horiba Jobin-Yvon) which provides a two-dimensional (512×512 pixels) photodetection of the seven input fibers. The horizontal and vertical dimensions respectively correspond to the spectral and directional resolutions. The CCD linearly converts the radiant energy into arbitrary counts.

2.3. Acquisition

The CCD camera is connected to a computer with an IEEE-488 interface and the acquisition line is run by the SpectraMax/32 software for Windows. The software partitions the CCD output into distinct areas in order to provide a spectrum for each active fiber. Five spectra are successively acquired and automatically averaged to calculate a representative one for each viewing direction. The integrating time which corresponds to the exposure time of the CCD sensors to light is chosen to maximize the detected signal without saturation. Prior to any acquisition, a measurement is systematically done with the shutter closed to subtract the dark current from the signal. Finally, we get a spectrum expressed in counts per second for each active fiber that needs to be calibrated.

2.4. Calibration of the sensors

We first conducted a spectral calibration using a mercury/argon lamp of known emission spectra. Because the sensors correspond to different areas of the CCD and different light pathways, this calibration was done one after the other. Then we compared their response when looking at the same source in the same configuration to derive calibration factors that do not depend on the wavelength. These factors permit comparison of signals acquired by different sensors.

2.5. Device output

The device is designed to perform comparative radiance measurements using a reference panel. To characterize this panel we set the illuminated and viewed area to 10 mm and 3 mm across at nadir, respectively. This way, except at grazing emerging angles $\theta_v > 70°$, the viewed area is fully illuminated and the measured signal V is proportional to the radiance L of the sample:

$$V(\theta_v, \phi_v, \lambda) = K \times L(\theta_v, \phi_v, \lambda) \quad (2)$$

where K is a calibration factor independent of the direction. For a leaf sample, we wish to average the optical properties of aerolaes (0.06 mm^2) and thus to increase the viewed area. We set it to 7 mm across at nadir. Since part of the latter may remain in the dark, K now depends on the direction:

$$V(\theta_v, \phi_v, \lambda) = K(\theta_v, \phi_v) \times L(\theta_v, \phi_v, \lambda) \quad (3)$$

where K accounts for geometrical effects. As we assume that these effects are not affected by the nature of the sample, the ratio of measured signals for a leaf sample and a reference sample with the same beams geometry equals the ratio of their radiances:

$$\frac{V_{leaf}(\theta_v, \phi_v, \lambda)}{V_{ref}(\theta_v, \phi_v, \lambda)} = \frac{L_{leaf}(\theta_v, \phi_v, \lambda)}{L_{ref}(\theta_v, \phi_v, \lambda)} \quad (4)$$

This ratio equals the biconical reflectance factor when the reference sample is lossless and Lambertian (Schaepman-Strub et al., 2006). Because the solid angles subtended by the source and the detectors are small and the corresponding light beams are parallel, it will be termed Bidirectional Reflectance Factor (BRF). It is used in the next section to derive the bidirectional optical properties of leaf samples.

3. Derivation of the bidirectional and directional–hemispherical reflectance and transmittance of a leaf sample

3.1. Definitions

Consider a lamp of irradiance dE (W m^{-2}) lighting an object in the direction (θ_s, ϕ_s). The radiance dL_r (W m^{-2} sr^{-1}) is emitted toward the upper hemisphere in the direction (θ_v, ϕ_v) in the solid angle $d\omega_v = \sin\theta_v d\theta_v d\phi_v$ at a given wavelength λ. The Bidirectional Reflectance Distribution Function (BRDF expressed in sr^{-1}) of the surface is defined by Nicodemus et al. (1977) as:

$$\mathrm{BRDF}(\theta_s, \phi_s, \theta_v, \phi_v, \lambda) = \frac{dL_r(\theta_s, \phi_s, \theta_v, \phi_v, \lambda)}{dE_i(\theta_s, \phi_s, \lambda)} \quad (5)$$

In the case of thin and translucent surfaces, one can also define the Bidirectional Transmittance Distribution Function (BTDF also expressed in sr^{-1}) by replacing the numerator of Eq. (5) with the radiance dL_t emitted toward the lower hemisphere:

$$\mathrm{BTDF}(\theta_s, \phi_s, \theta_v, \phi_v, \lambda) = \frac{dL_t(\theta_s, \phi_s, \theta_v, \phi_v, \lambda)}{dE_i(\theta_s, \phi_s, \lambda)} \quad (6)$$

To assess the amount of light reflected in a whole hemisphere, one calculates the Directional Hemispherical Reflectance Factor (DHRF) which is related to the BRDF by the following equation (Nicodemus et al., 1977):

$$\mathrm{DHRF}(\theta_s, \phi_s, \lambda) = \int \mathrm{BRDF}(\theta_s, \phi_s, \theta_v, \phi_v, \lambda)\cos\theta_v d\omega_v \quad (7)$$

where the integral covers the upper hemisphere. The same equation applies for the Directional Hemispherical Transmittance Factor (DHTF) where the BRDF is replaced by the BTDF and the upper hemisphere by the lower one.

3.2. BRDF of the reference panel

A Spectralon® diffuse reflectance panel was chosen to serve as an optical standard. Its bidirectional and hemispherical properties have been intensively studied in the frame of the

MISR mission (Bruegge et al., 2001; Haner et al., 1998). Its DHRF written ρ_H is constant between 400 nm and 900 nm and equals 0.99. For small illumination and viewing zenith angles, this reference panel is almost Lambertian, i.e., its BRDF equals $1/\pi$ whatever the wavelength and the direction. For larger viewing zenith angles, this relationship may be not verified and accurate measurements are required. By applying Eq. (7) we obtain:

$$\int \mathrm{BRDF}_{\mathrm{ref}}(\theta_s,\phi_s,\theta_v,\phi_v,\lambda)\cos\theta_v \mathrm{d}\omega_v = \int \frac{\mathrm{d}L_{r,\mathrm{ref}}(\theta_s,\phi_s,\theta_v,\phi_v,\lambda)}{\mathrm{d}E_i(\theta_s,\phi_s,\lambda)}\cos\theta_v \mathrm{d}\omega_v = \rho_H \quad (8)$$

Which leads to:

$$\mathrm{d}E_i(\theta_s,\phi_s,\lambda) = \frac{1}{\rho_H}\int \mathrm{d}L_{r,\mathrm{ref}}(\theta_s,\phi_s,\theta_v,\phi_v,\lambda)\cos\theta_v \mathrm{d}\omega_v \quad (9)$$

By substituting for $\mathrm{d}E_i$ in Eq. (5), with Eq. (9), results in:

$$\mathrm{BRDF}_{\mathrm{ref}}(\theta_s,\phi_s,\theta_v,\phi_v,\lambda) = \frac{\rho_H \times \mathrm{d}L_{r,\mathrm{ref}}(\theta_s,\phi_s,\theta_v,\phi_v,\lambda)}{\int \mathrm{d}L_{r,\mathrm{ref}}(\theta_s,\phi_s,\theta_v,\phi_v,\lambda)\cos\theta_v \mathrm{d}\omega_v} \quad (10)$$

Thus, although the reference panel is not Lambertian, its BRDF can be easily derived by summing the radiances measured with the SGP as described hereafter.

3.3. Leaf BRDF and BTDF

The device has been designed to measure the biconical reflectance factor defined as the ratio of the leaf radiance L_{leaf} to the reference panel radiance L_{ref} (see Eq. (4)). Dividing Eq. (5) applied to the leaf by Eq. (5) applied to the reference panel gives the leaf BRDF:

$$\mathrm{BRDF}_{\mathrm{leaf}}(\theta_s,\phi_s,\theta_v,\phi_v,\lambda) = \frac{\mathrm{d}L_{r,\mathrm{leaf}}(\theta_s,\phi_s,\theta_v,\phi_v,\lambda)}{\mathrm{d}L_{r,\mathrm{ref}}(\theta_s,\phi_s,\theta_v,\phi_v,\lambda)}\mathrm{BRDF}_{\mathrm{ref}}(\theta_s,\phi_s,\theta_v,\phi_v,\lambda) \quad (11)$$

And using Eq. (6) applied to the leaf instead of Eq. (5), gives the BTDF:

$$\mathrm{BTDF}_{\mathrm{leaf}}(\theta_s,\phi_s,\theta_v,\phi_v,\lambda) = \frac{\mathrm{d}L_{t,\mathrm{leaf}}(\theta_s,\phi_s,\theta_v,\phi_v,\lambda)}{\mathrm{d}L_{r,\mathrm{ref}}(\theta_s,\phi_s,\theta_v,\phi_v,\lambda)}\mathrm{BRDF}_{\mathrm{ref}}(\theta_s,\phi_s,\theta_v,\phi_v,\lambda) \quad (12)$$

Eqs. (11) and (12) are valid as long as the irradiance, the beam geometry, and directions do not change when replacing the reference with the sample. If the size of the studied surface varies with illumination and viewing angles, this variation must be the same for both targets. The measured $\mathrm{BRDF}_{\mathrm{ref}}$, $\mathrm{BRDF}_{\mathrm{leaf}}$ and $\mathrm{BTDF}_{\mathrm{leaf}}$ are approximations to the bidirectional quantities defined by Eqs. (10), (11) and (12) where the infinitesimal radiance $\mathrm{d}L$ (theoretical) is replaced by the finite radiance L (measured).

3.4. Directional summation

The calculation of the following integral is needed in Eq. (7) to derive the leaf DHRF from its BRDF:

$$\mathrm{DHRF}_{\mathrm{leaf}}(\theta_s,\phi_s) = \int\int \mathrm{BRDF}_{\mathrm{leaf}}(\theta_s,\phi_s,\alpha,\gamma)\cos\alpha\cos^2\gamma\,\mathrm{d}\alpha\,\mathrm{d}\gamma \quad (13)$$

The integral is written in the goniometer native coordinate system (α, γ) using relations given in Eq. (1) with $\beta=0$ for the sake of simplicity. In this way, the viewing directions (α_i, γ_i) form a regular grid and each of them corresponds to a value $\mathrm{BRDF}_{\mathrm{leaf},i}$. Applying a nearest neighbour interpolation to $\mathrm{BRDF}_{\mathrm{leaf}}(\alpha, \gamma)$ over the grid leads to a discrete sum easily calculable. The same method is used in Eq. (10) to calculate the BRDF of the reference panel.

4. Leaf BRDF and BTDF measurements

4.1. Bidirectional optical properties

The bidirectional reflectance and transmittance distribution functions of leaves have been determined during three experiments in the summer of 2000, the spring of 2003, and

Table 1
Description of the dataset

Year	Leaf species	D/M	Characteristics	R/T
2000	*Juglans regia* L. (walnut)	D		R
	Sorghum bicolor (L.) Moench (sorghum)	M		R
2003	*Acer pseudoplatanus* L. (sycamore maple)	D	Young and old leaves	R
	Corylus avellana (hazel)	D	Downy and undulating	R
	Fagus sylvatica L. (European beech)	D	Very undulating	R
	Phaseolus vulgaris (green bean)	D	Slightly undulating	R
	Prunus laurocerasus L. (cherry laurel)	D	Young and old leaves	R
2005	*Fagus sylvatica* L. (European beech)	D	Smooth, glossy	R, T
	Festuca arundinacea (tall fescue)	M	Very rough	R, T
	Glycine max (L.) Merr. (soybean)	D	Rough, young	R, T
	Juglans regia L. (walnut)	D	Smooth, old	R, T
	Prunus laurocerasus L. (cherry laurel)	D	Very smooth, glossy	R, T
	Vitis vinifera L. (vine grape)	D	Rough, young	R, T
	Zea mays L. (corn)	M	Very rough, young	R, T

D stands for Dicotyledon and M for Monocotyledon. R stands for BRDF and T for BTDF.

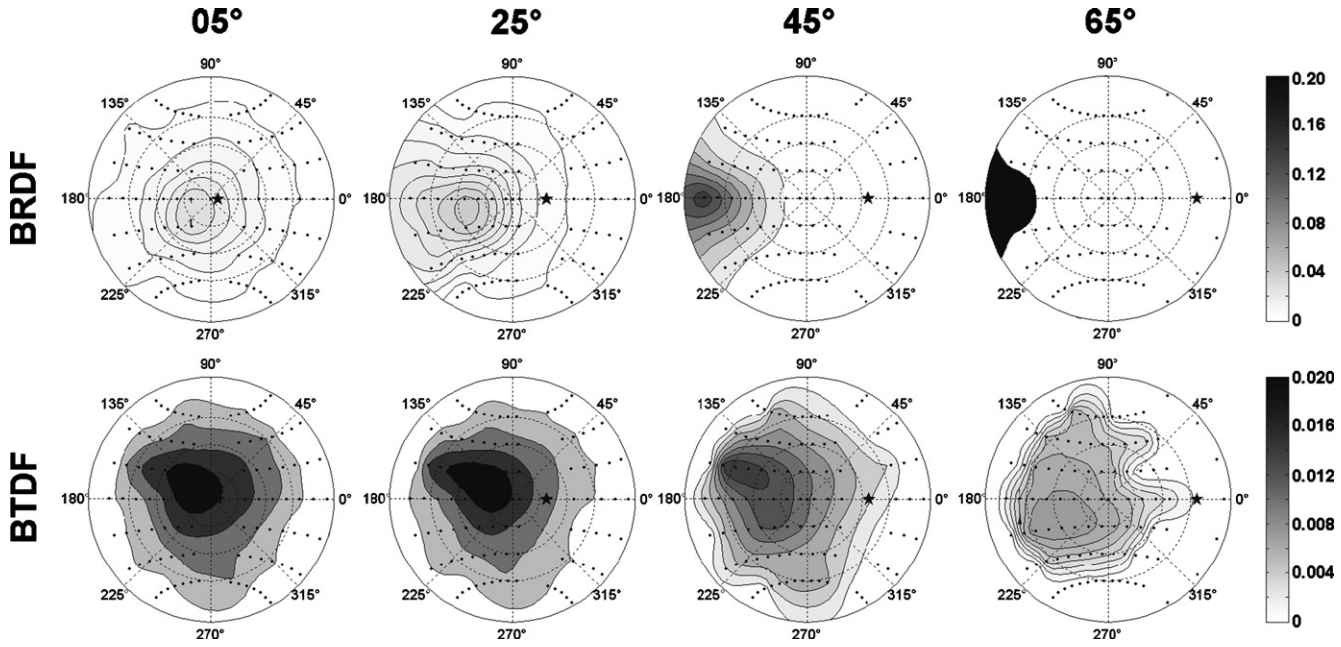

Fig. 5. Polar plot of the BRDF (top row) and BTDF (bottom row) in sr^{-1} of a beech leaf, the adaxial face of which is illuminated at 660 nm and {5°, 25°, 45°, 65°} incidence angles. The star and dots indicate the directions of illumination and viewing beams, respectively. Note different scales for the BRDF and the BTDF.

the summer of 2005. Eleven different species were selected that display a wide range of leaf anatomic structures (Monocots and Dicots) and surface features (Table 1). Besides the radiometric measurements, the chlorophyll content (in μg cm^{-2}), the water content (in g cm^{-2} or cm), and the dry matter content (in g cm^{-2}) were quantified for each leaf during the experiment of 2005. We also observed the mesophyll structure of some leaf species using an optical microscope. The protocol to measure the reflectance and transmittance of leaf samples is as follows:

(1) wait for the light source and spectrometer cooling system to stabilize over at least 30 min;
(2) set the illumination angle (position of the illumination fiber on the outer arc and angle β) and record it with the software;
(3) specify the number of viewing directions in the software;
(4) fix the reference panel on the sample holder;
(5) set the appropriate integration time in order to avoid saturating the CCD;
(6) and measure the radiance of the reference panel in the viewing directions specified at step (3).

Steps (4) through (6) are repeated with the leaf. When possible, we avoid illuminating the main veins and, for parallel-veined leaves like fescue and maize, the illumination direction is set perpendicular to the midrib. The whole procedure requires about 30 min for 200 reflection and transmission directions at a given illumination direction. The leaf is not illuminated between two acquisitions and its stem is kept in wet cellulose to prevent it from drying out.

For comparison, Fig. 5 shows the BRDF and BTDF at 660 nm of the adaxial (upper side) face of the European beech (*Fagus sylvatica* L.) leaf, illuminated from four incidence angles (θ_s=5°, 25°, 45°, 65°) indicated by the star on the polar plots. This species presents an intermediate condition between a glossy leaf (e.g., cherry laurel) and a pubescent one (e.g., hazel) as noted by Bousquet et al. (2005). The specular nature of the reflectance is evident: the BRDF shows a large anisotropy which increases as the light direction proceeds away from nadir. The maxima range from 0.03 sr^{-1} at θ_s=5° to 0.45 sr^{-1} at θ_s=65°, i.e., 15 times greater. The BTDF are much more isotropic than the BRDF although one can clearly observe an increase in transmittance in proximity of the principal plane as noticed earlier by Walter-Shea et al. (1989), Brakke et al. (1989), and Brakke (1994).

The leaf surface is sometimes crinkly, veined, or convex so that the BRDF/BTDF present some unexpected features. For instance, the fescue grass leaf characterized by parallel secondary veins between the midrib and leaf edge has one maximum in forward and one in backward direction (Fig. 6a) because the veins were perpendicular to the principal plane. Metzner (1957) and Grant et al. (1993) previously mentioned that topographical undulations might redirect a significant

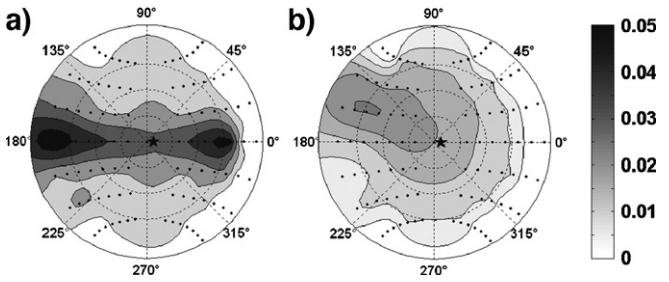

Fig. 6. Polar plot of the BRDF in sr^{-1} of (a) a fescue grass leaf and (b) a walnut leaf, the adaxial faces of which are illuminated at 660 nm and 5° incidence angle.

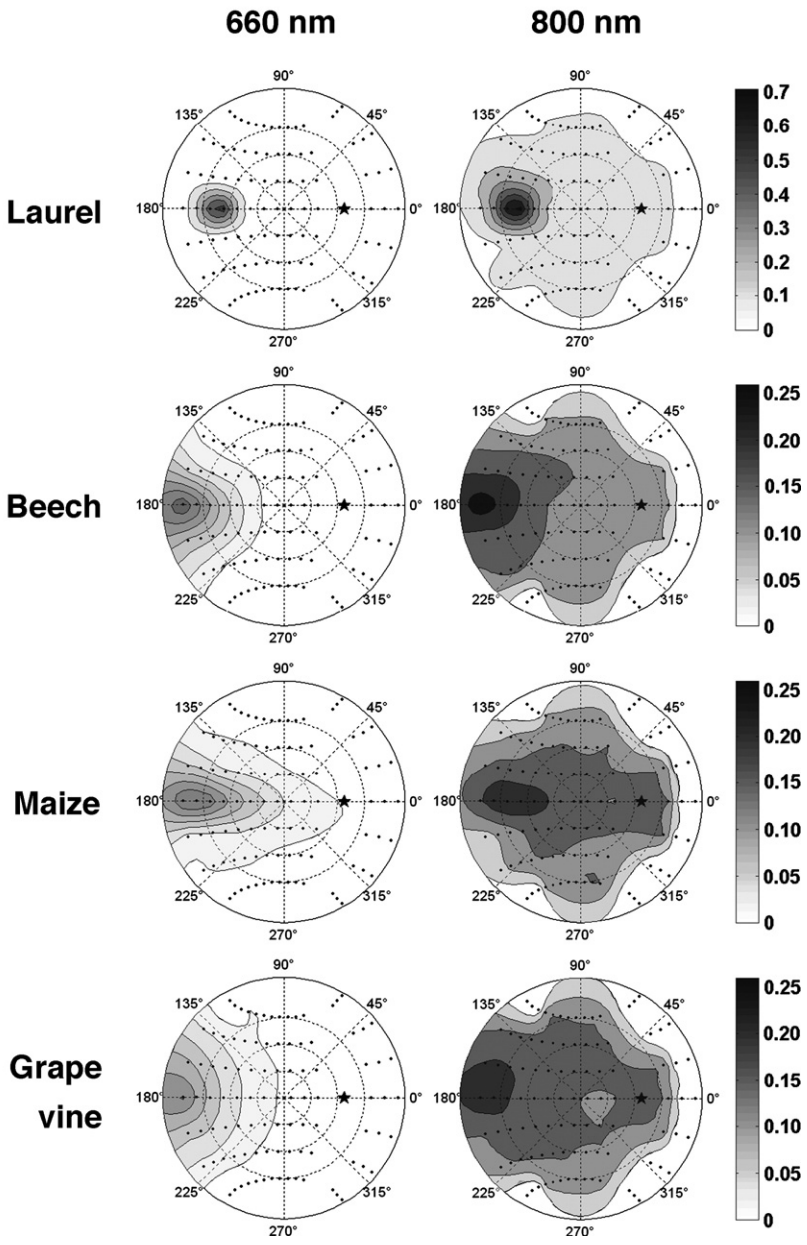

Fig. 7. Polar plot of the BRDF in sr^{-1} of laurel, beech, maize, and grape vine leaves, the adaxial faces of which are illuminated at 660 nm and 800 nm and 45° incidence angle.

part of reflected light toward the sensor. Moreover, the maximum reflectance peak of the walnut leaf (Fig. 6b) is out of the principal plane besides the specular direction. As observed by Brakke et al. (1989), it is difficult to maintain some leaves perfectly flat in the sample holder. Problems of undulation which appeared to increase the reflectance out of

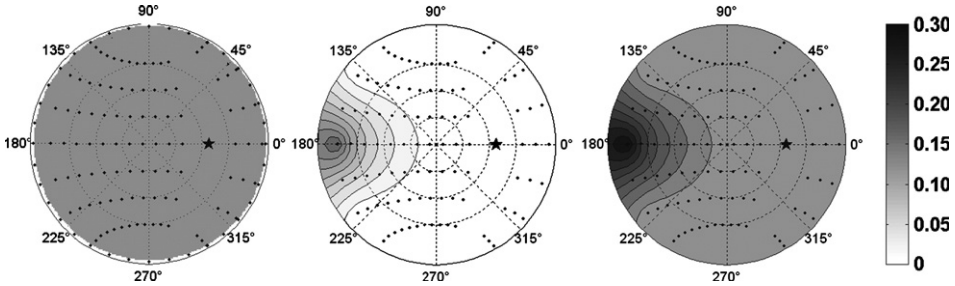

Fig. 8. Polar plot of the modeled BRDF in sr^{-1} of a beech leaf at 800 nm and 45° incidence: diffuse (left), specular (middle), and diffuse + specular (right) components.

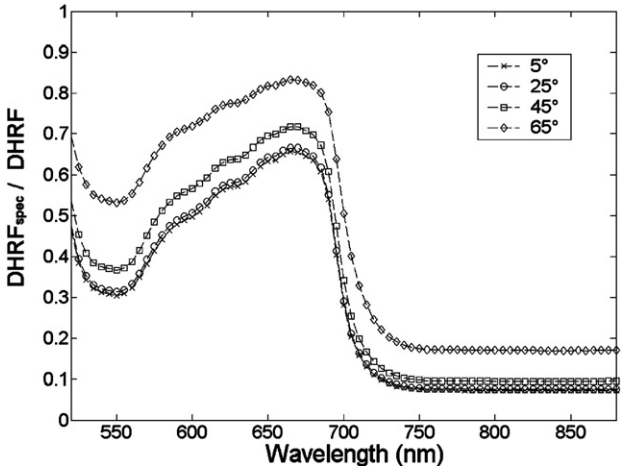

Fig. 9. Ratio of the specular component of the DHRF to the total DHRF for the beech leaf illuminated at 5°, 25°, 45° and 65° incidence angles.

the specular direction have been also reported in other studies (Woolley, 1971).

4.2. About the specular peak

The shape, position and magnitude of the specular peak, as well as its contribution to directional–hemispherical reflectance, have not been well quantified in the literature. A possible reason is that most of the studies present measurements in the principal plane (Breece & Holmes, 1971; Ross, 1981; Woolley, 1971). Fig. 5 nicely illustrates the expected increase of magnitude with increasing illumination zenith angle, as mentioned earlier. The BRDF of cherry laurel (*Prunus laurocerasus* L.), European beech (*Fagus sylvatica* L.), maize (*Zea mays* L.), and grape vine (*Vitis vinifera* L.) leaves plotted at two wavelengths and 45° incidence in Fig. 7 show a wide variety of shapes and magnitudes. The specular lobe is definitely not restrained in the principal plane. It is more easily identified in the visible than in the near-infrared because of low diffuse background levels. The narrowest lobe is observed for laurel, the surface of which looks glossy, and the largest is observed for the grape vine which has a matted finish to the naked eye. This widening is generally due to pubescence on the leaf surface which tends to scatter radiation in off-specular directions, or to a thinner wax layer which reveals the roughness of the epidermis cells. For parallel-veined leaves, the surface roughness is greater in the direction perpendicular to the veins. As observed for maize, the greatest widening occurs in the direction of the greatest surface roughness.

A model to investigate the geometry of the specular lobe can add insight into leaf bidirectional reflectance properties. In the paper recently published by Bousquet et al. (2005), the BRDF is assumed to be the sum of a diffuse component $\mathrm{BRDF}_{\mathrm{diff}}(\lambda)$ independent of the directions and a specular component $\mathrm{BRDF}_{\mathrm{spec}}(\theta_s, \phi_s, \theta_v, \phi_v)$ independent of the wavelength:

$$\mathrm{BRDF}_{\mathrm{diff}}(\lambda) + \mathrm{BRDF}_{\mathrm{spec}}(\theta_s, \phi_s, \theta_v, \phi_v) = \mathrm{BRDF}(\theta_s, \phi_s, \theta_v, \phi_v, \lambda) \quad (14)$$

The three variables of the model are the refractive index n, the surface roughness parameter σ, and the Lambert parameter $k_L(\lambda)$ linked to light absorption and scattering within the leaf blade, thus wavelength dependent. Model inversions that we performed on the BRDF presented in Figs. 5 and 7 resulted in $n=1.42$, $\sigma=0.32$, and $k_L(\lambda)$ ranging from 0.01 to 0.39 for beech; $n=1.51$, $\sigma=0.12$, and $k_L(\lambda)$ ranging from 0.01 to 0.51 for laurel. These values were then used in direct mode to determine the proportion of the specular lobe in the leaf BRDF. Fig. 8 illustrates the modeled distribution of diffuse and specular light reflected by the beech leaf at 800 nm and 45° incidence. Quantitative analysis is then feasible. By substituting Eq. (14) into Eq. (7) one can first calculate the diffuse and specular components of the DHRF:

$$\mathrm{DHRF}_{\mathrm{diff}}(\lambda) + \mathrm{DHRF}_{\mathrm{spec}}(\theta_s, \phi_s) = \mathrm{DHRF}(\theta_s, \phi_s, \lambda) \quad (15)$$

$\mathrm{DHRF}_{\mathrm{diff}}(\lambda)$ simply equals $k_L(\lambda)$ while $\mathrm{DHRF}_{\mathrm{spec}}(\theta_s, \phi_s)$ is numerically computed because no analytical expression is known. The spectral variation of the ratio of $\mathrm{DHRF}_{\mathrm{spec}}(\theta_s, \phi_s)$ to $\mathrm{DHRF}(\theta_s, \phi_s, \lambda)$ corresponding to the beech leaf has been plotted in Fig. 9 at four incidence angles. It is noticeable that the specular lobe represents only 8% of the whole amount of reflected radiation in the near infrared, 30–50% in the green, and up to 60–80% in the red (up to 90% for laurel). This is an important result in terms of light scattering and absorption within a plant canopy: the near infrared radiation is intensively scattered but since the specular lobe is reduced compared to the diffuse background signal, its contribution may be neglected. On the contrary, the visible light is intensively absorbed by the leaf photosynthetic pigments so that the contribution of the specular lobe may also quickly disappear. Finally, increasing the incidence angle tends to increase this ratio on the whole spectrum.

We also evaluated the solid angle which circumscribes the specular lobe. For each incidence angle θ_s we calculated the maximum of $\mathrm{BRDF}_{\mathrm{spec}}(\theta_s, \phi_s, \theta_v, \phi_v)$, the related zenith viewing angle θ_v and the solid angle Ω_{spec} corresponding to 90% of the amount of specularly reflected light $\mathrm{DHRF}_{\mathrm{spec}}(\theta_s, \phi_s)$. Table 2 is informative about the shape, position and magnitude of the specular lobe. Predictably enough, the width of the lobe decreases with illumination angle while its magnitude increases. The specular lobe represents 37% of the upper hemisphere for the beech leaf lit at 5° and 2.7% for the

Table 2
Characteristics of the specular lobe as a function of the incidence angle

Incidence angle θ_s		5°	25°	45°	65°
Maximum of $\mathrm{BRDF}_{\mathrm{spec}}$ (sr^{-1})	Beech	0.024	0.031	0.185	3.11
	Laurel	0.223	0.274	0.576	4.96
Viewing angle θ_v of the maximum	Beech	7°	42°	80°	89°
	Laurel	5°	26°	48°	75°
Solid angle of the specular lobe Ω_{spec} (sr)	Beech	2.35	2.29	1.61	0.79
	Laurel	0.41	0.37	0.30	0.17
$\mathrm{DHRF}_{\mathrm{spec}}$	Beech	0.030	0.032	0.040	0.079
	Laurel	0.041	0.042	0.052	0.121

laurel leaf lit at 65°. The maximum peak is not exactly in the specular direction as one expects from a mirror-like surface, but at greater viewing angles, especially for beech. This roughness effect has been observed and explained for artificial target by Torrance and Sparrow (1967).

4.3. Directional–hemispherical optical properties

From the measured BRDF or BTDF one can derive the directional–hemispherical reflectance (DHRF) or transmittance (DHTF) by numerical integration over the upper or lower hemisphere. The estimation of these quantities, which is quite accurate for Lambertian BRDF and BTDF, tends to deteriorate with increasing anisotropy. In particular, the strong and narrow specular peak observed for illumination angles of 45° and 65° is likely to cause a wrong estimation due to sampling artefacts. Fig. 10 shows the DHRF and DHTF of two leaves at four illumination angles. The DHRF obviously increases while the DHTF decreases with the angle of incidence, as observed in previous studies (Brandt and Tageyeva cited in Brakke et al., 1989; Ross, 1981; Walter-Shea et al., 1989).

5. Conclusion and discussion

The primary objective of this study was to present a new apparatus intended to measure the leaf bidirectional optical properties, a subject that is not well-documented compared to spectral properties, and to provide a better understanding of their determinism. The spectral and directional sampling of the BRDF and BTDF presented in this paper has been rarely reached before. Some studies are limited to reflectance measurements; others gather full spectra acquired in a few directions or cover the whole hemisphere but only at a few wavelengths. Most of them show scattering data in the principal plane, which does not allow to separate the diffuse component from the specular component and to grasp the three-dimensional shape of the latter. We should mention that the directional sampling of our SGP in the forward direction might be inadequate to finely characterize the specular peak whose shape is narrow for some plant species. A device equipped with stepper motors would be better designed to obtain such information by covering some areas more densely. In the same way we lack data at small phase angles due to alignment and occultation problems: to our knowledge, the opposition effect has only been observed by Howard (1969) on four

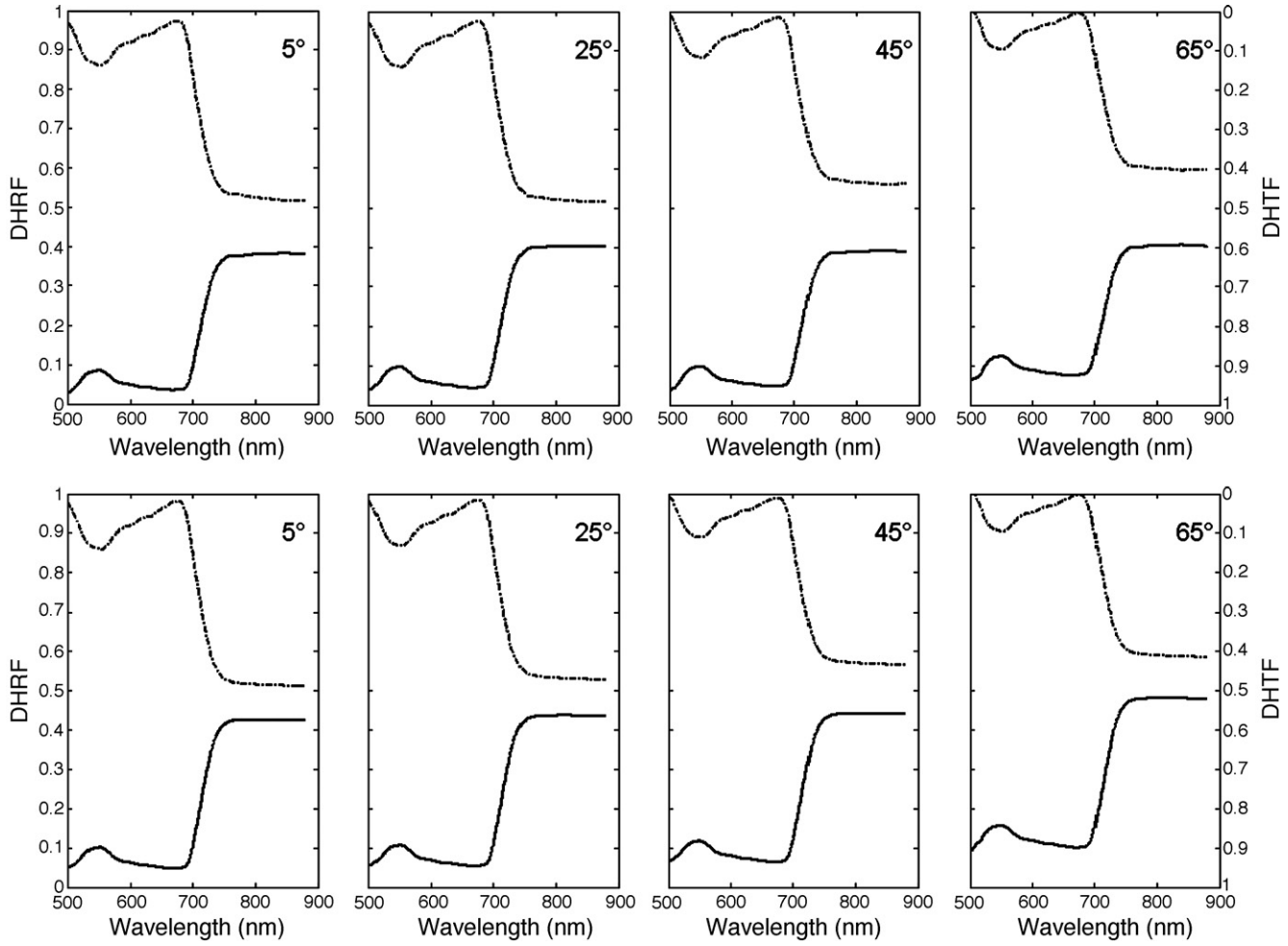

Fig. 10. DHRF (solid line) and DHTF (dotted line, reverse scale) of beech (top) and grape vine (bottom) as a function of the wavelength for four illumination zenith angles.

Eucalyptus leaves. He clearly showed an increase in the luminance factor between 4° and 0° phase angles at 45° incidence. Instruments suited to such measurements exist (Buratti et al., 1988; White et al., 1998) and could be used to initiate new studies to confirm this result. Other improvements in the design of the SGP are likely to decrease the uncertainties, for instance the use of a reference panel similar to the leaf in thickness and scattering features or the investigation of angular error propagation in rotation systems, which basically depend on the apparatus configuration (Torrington, 2003).

The published literature on leaf BRDF and BTDF is largely scarce and qualitative. For many applications it is however important to have quantitative values on leaf bidirectional radiative properties. The SGP could be used to build a database of different crop and natural vegetation leaf BRDF and BTDF. As seen earlier, there is large variability in leaf BRDF of different species but also within different species of the same genus (Howard, 1971). Due to a lack of measurements and to unsuitable canopy reflectance models, it has become an accepted fact in the scientific community that leaf bidirectional optical properties had little influence on canopy BRDF. However, only a few attempts were made to include leaf specular reflectance in 1D plant canopy reflectance models (Nilson & Kuusk, 1989; Reyna & Badhwar, 1985; Ross & Marshak, 1989; Vanderbilt & Grant, 1985). The development of outstanding 3D radiative transfer codes capable of decomposing a leaf in hundreds of facets and to allot them non-Lambertian optical properties should open new vistas in ecophysiology and remote sensing. For instance Chelle (2006) recently performed simulations of radiation absorption by dense, homogeneous crop canopies using a Monte Carlo ray tracing code and concluded that the Lambertian approximation might be suitable for photosynthesis or photomorphogenesis studies. Intuitively one can admit this approximation for dense canopies but certainly not for sparse ones, e.g., during the early stages of plant development, where the *n*-order scattering is limited. Considering hemispherical fluxes in plant functioning models is rough because leaves (plan-like), stems (cylinder-like), and apexes (hemisphere-like) definitely redirect light onto special directions. Then the directional and spectral irradiance on plant organs becomes an important parameter of the phyllosphere (Chelle, 2005) because some organs have small fields-of-view, i.e., they receive energy from their surrounding environment only within a small angle.

Besides the changes meant to improve the SGP functioning, it would be interesting to measure the directional chlorophyll fluorescence of green leaves in the frame of the FLEX (Fluorescence Explorer) program of the European Space Agency. About 15 years ago, Pedrini et al. (personal communication) from the Joint Research Centre (Ispra, Italy) made such measurements on philodendron and tobacco leaves illuminated by a laser beam at 632.8 nm. They found isotropic fluorescence emission properties, as expected, but never published their results because of considerable variability, depending on the area of the leaf blade which was analyzed. We are thinking of repeating the same experiment by replacing the light source by a larger laser beam which may yield better results. Finally, although it would require changing the spectrometer and the optical fibers, the extension of the measurements to the shortwave infrared would provide very valuable information about the spectral variation of the refractive index of leaf surface materials in this domain.

Acknowledgment

This work was supported by the Programme National de Télédétection Spatiale (PNTS), the GDR 1536 FLUOVEG (Fluorescence of Vegetation), and the Institut National de la Recherche Agronomique (INRA). Many thanks to Susan L. Ustin (U.C. Davis) for reading and correcting the paper.

References

Ballaré, C. L., Sánchez, R. A., Scopel, A. L., Casal, J. J., & Ghersa, C. M. (1987). Early detection of neighbor plants by phytochrome perception of spectral changes in reflected sunlight. *Plant, Cell and Environment*, *10*, 551–557.

Bousquet, L., Lachérade, S., Jacquemoud, S., & Moya, I. (2005). Leaf BRDF measurement and model for specular and diffuse component differentiation. *Remote Sensing of Environment*, *98*, 201–211.

Brakke, T. W. (1994). Specular and diffuse components of radiation scattered by leaves. *Agricultural and Forest Meteorology*, *71*, 283–295.

Brakke, T. W., Smith, J. A., & Harnden, J. M. (1989). Bidirectional scattering of light from tree leaves. *Remote Sensing of Environment*, *29*, 175–183.

Breece, H. T., & Holmes, R. A. (1971). Bidirectional scattering characteristics of healthy green soybean and corn leaves *in vivo*. *Applied Optics*, *10*, 119–127.

Bruegge, C., Chrien, N., & Haner, D. (2001). A Spectralon BRF data base for MISR calibration applications. *Remote Sensing of Environment*, *76*, 354–366.

Buratti, B. J., Smythe, W. D., Nelson, R. M., & Gharakhani, V. (1988). Spectrogoniometer for measuring planetary surface materials at small phase angles. *Applied Optics*, *27*, 161–165.

Chelle, M. (2005). Phylloclimate or the climate perceived by individual plant organs: What is it? How to model it? What for? *New Phytologist*, *166*, 781–790.

Chelle, M. (2006). Could plant leaves be treated as Lambertian surfaces in dense crop canopies to estimate light absorption? *Ecological Modelling*, *198*, 219–228.

Combes D. (2002). Comparaison de modèles de transferts radiatifs pour simuler la distribution du rayonnement actif sur la morphogénèse (MAR) au sein d'un peuplement végétal à l'échelle locale. Thèse de Doctorat en Physique de l'Atmosphère, Université Blaise Pascal, Clermont Ferrand (France), 175 pp.

Grant, L., Daughtry, C. S. T., & Vanderbilt, V. C. (1993). Polarized and specular reflectance variation with leaf surface features. *Physiologia Plantarum*, *88*, 1–9.

Haner, D. A., McGuckin, B. T., Menzies, R. T., Bruegge, C. J., & Duval, V. (1998). Directional–hemispherical reflectance for Spectralon by integration of its bidirectional reflectance. *Applied Optics*, *37*, 3996–3999.

Howard, J. A. (1969). Increased luminance in the direction of reflex reflexion — A recently observed natural phenomenon. *Nature*, *224*, 1102–1103.

Howard, J. A. (1971). Luminance and luminous intensity indicatrices of isolateral leaves. *Applied Optics*, *10*, 2354–2360.

Jacques, S. L., Alter, C. A., & Prahl, S. A. (1987). Angular dependence of HeNe laser light scattering by human dermis. *Lasers in the Life Sciences*, *1*, 309–334.

Metzner, P. (1957). Zur Optik der Blattoberflächen. *Die Kulturpflanze*, *5*, 221–239.

Myneni, R. B., & Ross, J. (1991). *Photon–vegetation interactions: Applications in optical remote sensing and plant ecology.* New York: Springer-Verlag 565 pp.

Myneni, R. B., Ross, J., & Asrar, G. (1989). A review on the theory of photon transport in leaf canopies. *Agricultural and Forest Meteorology*, *45*, 1–153.

Nicodemus, F. E., Richmond, J. C., Hsia, J. J., Ginsberg, I. W., & Limperis, T. (1977). *Geometrical considerations and nomenclature for reflectance.* Washington, DC: National Bureau of Standards, US Department of Commerce NBS MN-160, October 1977, 52 pp.

Nilson, T., & Kuusk, A. (1989). A reflectance model for the homogeneous plant canopy and its inversion. *Remote Sensing of Environment*, *27*, 157−167.

Okayama, H. (1996). How different are the indicatrixes of the leaves of various woody plant species? *Applied Optics*, *35*, 3250−3254.

Pont, S. C., & Koenderink, J. J. (2003). Split off-specular reflection and surface scattering from woven materials. *Applied Optics*, *42*, 1526−1533.

Reyna, E., & Badhwar, G. D. (1985). Inclusion of specular reflectance in vegetative canopy models. *IEEE Transactions on Geoscience and Remote Sensing*, *23*, 731−736.

Ross, J. (1981). *The radiation regime and architecture of plant stands.* Kluwer Academic Publishers 420 pp.

Ross, J., & Marshak, A. (1989). The influence of leaf orientation and the specular component of leaf reflectance on the canopy bidirectional reflectance. *Remote Sensing of Environment*, *27*, 251−260.

Sarto, A. W., Woldemar, C. M., & Vanderbilt, V. C. (1989). POlarized Light Angle Reflectance instrument I polarized incidence (POLAR:I). *Proc. polarization considerations for optical systems II, San Diego (CA), 9–11 AugustSPIE*, *Vol. 1166*. (pp. 220−230).

Sasse, C. (1993). Development of an experimental system for optical characterization of large arbitrarily shaped particles. *Review of Scientific Instruments*, *64*, 864−869.

Schaepman-Strub, G., Schaepman, M. E., Painter, T. H., Dangel, S., & Martonchik, J. V. (2006). Reflectance quantities in optical remote sensing — Definitions and case studies. *Remote Sensing of Environment*, *103*, 27−42.

Smith, H. (1982). Light quality, photoperception, and plant strategy. *Annual Review of Plant Physiology*, *33*, 481−518.

Stavenga, D. G. (2002). Colour in the eyes of insects. *Journal of Comparative Physiology. A, Sensory, Neural, and Behavioral Physiology*, *188*, 337−348.

Torrance, K. E., & Sparrow, E. M. (1967). Theory for off-specular reflection from roughened surfaces. *Journal of the Optical Society of America*, *57*, 1105−1114.

Torrington, G. K. (2003). Propagation of angular errors in two-axis rotation systems. In A. E. Hatheway (Ed.), *Proc. SPIE optomechanics*, *Vol. 5176*. (pp. 168−178) Bellingham WA, USA.

Vanderbilt, V. C., & Grant, L. (1985). Plant canopy specular reflectance model. *IEEE Transactions on Geoscience and Remote Sensing*, *23*, 722−730.

Vanderbilt, V. C., & Grant, L. (1986). Polarization photometer to measure bidirectional reflectance factor R(55°, 0°; 55°, 180°) of leaves. *Optical Engineering*, *25*, 566−571.

Von Schönermark, M., Geiger, B. & Röser, H. P. (Eds.). (2004). *Reflection properties of vegetation and soil, with a BRDF data base.* Berlin: Wissenschaft and Technik Verlag 352 pp.

Walter-Shea, E. A., Norman, J. M., & Blad, B. L. (1989). Leaf bidirectional reflectance and transmittance in corn and soybean. *Remote Sensing of Environment*, *29*, 161−174.

White, D. R., Saunders, P., Bonsey, S., Van de Ven, J., & Edgar, H. (1998). Reflectometer for measuring the bidirectional reflectance of rough surfaces. *Applied Optics*, *37*, 3450−3454.

Woolley, J. T. (1971). Reflectance and transmittance of light by leaves. *Plant Physiology*, *47*, 656−662.